

1 Monte Carlo sampling for error propagation in linear 2 regression and applications in isochron geochronology

3 Yang Li^{1,2,3}, Shuang Zhang³, Richard Hobbs², Camila Caiado⁴, Adam D. Sproson^{2,5},
4 David Selby², Alan D. Rooney³

5 ¹State Key Laboratory of Lithospheric Evolution, Institute of Geology and Geophysics,
6 Chinese Academy of Sciences, Beijing, 10029, China

7 ²Department of Earth Sciences, Durham University, Durham, DH1 3LE, UK

8 ³Department of Geology and Geophysics, Yale University, New Haven, Connecticut, 06511,
9 USA

10 ⁴Department of Mathematical Sciences, Durham University, Durham, DH1 3LE, UK

11 ⁵Atmosphere and Ocean Research Institute, The University of Tokyo, 5-1-5 Kashiwa-no-ha,
12 Kashiwa 275-8564, Japan

13 Corresponding author: Yang Li (geoliy@mail.iggcas.ac.cn; cugliyang@126.com)

14 Key points:

- 15 • Full propagation of uncertainties from experimental sources and underlying
16 assumptions in linear regression and their implications in isochron dating;
- 17 • An ability to incorporate geological information;

18 **Abstract**

19 Geochronology is essential for understanding Earth's history. The availability of
20 precise and accurate isotopic data is increasing; hence it is crucial to develop transparent and
21 accessible data reduction techniques and tools to transform raw mass spectrometry data into
22 robust chronological data. Here we present a Monte Carlo sampling approach to fully propagate
23 uncertainties from linear regressions for isochron dating. Our new approach makes no prior
24 assumption about the causes of variability in the derived chronological results and propagates
25 uncertainties from both experimental measurements (analytical uncertainties) and underlying
26 assumptions (model uncertainties) into the final age determination. Using synthetic examples,
27 we find that although the estimates of the slope and y-intercept (hence age and initial isotopic
28 ratios) are comparable between the Monte Carlo method and the benchmark "Isoplot"
29 algorithm, uncertainties from the later could be underestimated by up to 60%, which are likely
30 due to an incomplete propagation of model uncertainties. An additional advantage of the new
31 method is its ability to integrate with geological information to yield refined chronological
32 constraints. The new method presented here is specifically designed to fully propagate errors
33 in linear regressions especially in geochronological applications involves linear regressions
34 such as Rb-Sr, Sm-Nd, Re-Os, Pt-Os, Lu-Hf, U-Pb (with discordant points), Pb-Pb and Ar-Ar.

36 **Keywords**

37 Linear regression; Isochron; Geochronology; Uncertainty Propagation; Monte Carlo; Isoplot

1. Introduction

Geochronology is an essential aspect of Earth sciences, and advances in this field have resulted in many breakthroughs in understanding the history of our solar system and the evolution of life on Earth [1]. In general, extracting geologically meaningful ages from rocks and minerals starts with sample collection, followed by sample processing, and isotopic ratio measurements via mass spectrometry. The raw isotopic ratios generated by mass spectrometers then need to be transformed into atomic ratios, and eventually into chronological dates with propagation of associated uncertainties [e.g., 2, 3]. Over the past three decades, a great number of analytical innovations and instrumentation advances have emerged, which gave rise to unprecedented levels of accuracy and precision for isotopic ratio measurements as well as pioneering new radiometric systems for questions ranging from early solar system evolution to Anthropocene climate change. Advances in the precision and accuracy as well as the expansion of available geochronometers has been facilitated by a combination (often iteratively) of better analytical approaches and robust, transparent and accessible data reduction tools [e.g., 4, 5-13]. To more fully harness these technical improvements, it is critical to concomitantly develop data reduction techniques and appropriate visualization methods. Although there have been significant progresses made in data reduction techniques for U-Th-Pb and Ar-Ar systems [3, 6, 7, 14-20], fewer advances have been seen in isochron dating, a method utilized for systems including Re-Os.

Isochron dating is based on linear regression in which one determines the slope, y-intercept and associated uncertainties of the best fitting line to the parent and daughter isotopic ratios (including their uncertainties and error correlations). The fundamental assumptions behind isochron dating include: (1) all co-genetic samples have near-identical initial daughter isotopic compositions; (2) samples begin accumulating daughter isotopes via radiogenic decay at the same time; (3) these samples remain closed in terms of both parent and daughter isotopes

1
2
3 63 following the accumulation of the daughter isotope. A further requirement is that these samples
4
5 64 should have variable parent isotope (or daughter isotope) ratios to define a line. This linear
6
7
8 65 regression is routinely carried out by the “Isoplot” program that is based on a Microsoft Excel
9
10 66 macro [2, 21] and includes York’s algorithm [22-24]. This algorithm performs a least-squares
11
12 67 fit to data with normally distributed but correlated uncertainties, and assumes that the data
13
14 68 points lie along a straight line (isochron) and offsets from this line are due to imperfect
15
16 69 measurements, otherwise known as analytical uncertainties. In reality however, the data points
17
18 70 might not fall on a straight line even if they could be measured perfectly because of differences
19
20 71 in initial isotopic composition, varying ages and/or open system behavior, which we will refer
21
22 72 as model uncertainties. To address this, the “Isoplot” program uses two different techniques
23
24 73 (additional options are discussed below) for error propagation and decides which one to use
25
26 74 based on the probability of how well the data “fits” to the line. If the probability of fit is
27
28 75 satisfactory, “Isoplot” assumes that analytical uncertainty is the only cause of scatter and uses
29
30 76 York’s algorithm to propagate only analytical uncertainties to produce a so-called Model 1 age.
31
32 77 If the fit of the data to a common line is not satisfactory resulting in a violation of York’s
33
34 78 assumption (i.e., in the case of over-dispersion), “Isoplot” uses an adapted regression that
35
36 79 accounts for an unknown but normally distributed variation in the initial isotopic ratios of the
37
38 80 samples [2, 25], producing a Model 3 age. Though the users can choose the cutoff value
39
40 81 between the two Models (between 0.05 and 0.3 with a default of 0.15), in the absence of
41
42 82 additional geologic constraints, there is no standard criteria to choose this cutoff value, which
43
44 83 can lead to inconsistencies in chronological results if this value is not properly documented.
45
46
47
48
49

50
51 84 “Isoplot” also offers a Model 2 solution in which case equal weights and zero error
52
53 85 correlations are assigned to the samples, as opposed to those used in Model 1 and Model 3
54
55 86 where each sample has a weighting proportional to the inverse square of its analytical
56
57 87 uncertainties (also accounts the error correlation). When the assumption that residuals
58
59
60

1
2
3 88 (observed scatter) of the data-points from a straight line have a normal (Gaussian) distribution
4
5 89 is invalid, “Isoplot” has an option called “Robust regression” which makes no assumptions
6
7
8 90 about the cause(s) of the observed scatter of the data from a straight line. We do not discuss
9
10 91 these two options further as they are rarely used and beyond the scope of this study.

11
12 92 As pointed out by Ludwig [26], uncertainty determined by Monte Carlo sampling is the
13
14 93 most reliable approach, therefore in this paper we propose an method to determine the slope,
15
16 94 y-intercept and their uncertainties, based on Monte Carlo sampling and simple linear regression.
17
18 95 Unlike the Monte Carlo method in York et al., (2004) [24], the proposed method here
19
20 96 propagates not only analytical uncertainties, but also uncertainties arising from the underlying
21
22 97 assumptions (model uncertainties). This approach differs from Model 1 and Model 3 solutions
23
24 98 from Isoplot as our new method propagates uncertainties in a consistent manner regardless of
25
26 99 the probability of fit and hence avoids subjective choosing of the cut-off value discussed above.
27
28
29
30
31 100 Our method can be applied to data with any goodness of fit and distinguishes between
32
33 101 analytical and model uncertainties. This paper discusses three key aspects: (1) the Monte Carlo
34
35 102 based method; (2) the examination of differences and similarities to Isoplot; and (3) the use of
36
37 103 a synthetic dataset to demonstrate the potential to integrate independent geological information
38
39
40 104 for refined chronologic constraints.

41 42 43 105 **2. Monte Carlo simulation**

44 45 46 106 2.1 Experimental data and their uncertainties

47
48
49 107 The parent and daughter isotopic ratios (X, Y) of a sample are measured experimentally,
50
51 108 with their uncertainties (δX , δY) inherited from the analytical procedure. Additionally, the
52
53 109 uncertainties of the parent and daughter isotopic ratios are typically correlated due to the
54
55 110 utilization of a common isotope used to convert absolute atomic numbers into isotopic ratios
56
57
58 111 (e.g., ^{86}Sr in $^{87}\text{Rb}/^{86}\text{Sr}$ and $^{87}\text{Sr}/^{86}\text{Sr}$; ^{144}Nd in $^{147}\text{Sm}/^{144}\text{Nd}$ and $^{143}\text{Nd}/^{144}\text{Nd}$), which is quantified
59
60

1
2
3 112 by a correlation coefficient [denoted by ρ or rho; 27]. Experimental data with the same parent
4
5 113 and daughter isotopic ratios and uncertainties, but variable error correlations are graphically
6
7 114 illustrated in [Figure 1A](#) as error ellipses at the 2-sigma level (all uncertainties are presented at
8
9 the 2-sigma level in absolute values unless otherwise stated). By definition, a high error
10 115 correlation indicates that the sources of δX and δY are predominately from one contributor,
11
12 116 which for isotope geochemistry is likely to be caused by the analytical uncertainty of the stable
13
14 117 isotope used to convert absolute atomic numbers into isotopic ratios. As emphasized by Ludwig
15
16 118 [26] and illustrated in [Figure 1A](#), the 2-sigma ellipses including error correlation extend farther
17
18 119 than the 2-sigma range of δX and δY , which is a non-intuitive characteristic of joint
19
20 120 distributions. As such, excluding error correlations for linear regressions will yield an incorrect
21
22 121 uncertainty for the slope and its uncertainty [28]. Hence it is critical to report and use accurate
23
24 122 error correlations for the experimental data in all geochronological studies which can be
25
26 123 estimated through differentiation and observation [2]. The analytical uncertainties with error
27
28 124 correlation can also be presented as probability density functions (PDFs, [Fig. 1B](#)). This
29
30 125 probability density function is the basis for the resampling process used in our Monte Carlo
31
32 126 method.
33
34
35
36
37
38
39

40 128 2.2 Propagation of analytical uncertainties

41
42
43 129 We demonstrate the principles of our Monte Carlo based technique using a synthetic
44
45 130 example consisting of five samples. The parent and daughter isotopic ratios and associated
46
47 131 uncertainties including error correlations of the five samples are graphically illustrated in
48
49 132 [Figure 2A](#) as error ellipses. To propagate analytical uncertainties, we perform the following
50
51 133 steps:
52
53

- 54 134 1. for each of the five samples, we randomly select a coordinate from its
55
56 135 corresponding probability density function as that defined in [Figure 1B](#). Each
57
58
59
60

1
2
3 136 sampled coordinate is considered to be a pair of absolute values without
4
5 137 uncertainty (Fig. 2A);
6
7
8 138 2. once a coordinate has been selected for each of the five samples, the parameters
9
10 139 (slope and y-intercept) of the regression line are determined (Fig. 2A) following
11
12 140 a least-square estimation [29]. The slope and y-intercept of this regression line
13
14 141 is plotted in Figure 2B;
15
16
17 142 3. repeating steps 1 and 2 yields a distribution representing the probability of slope
18
19 143 and y-intercept of the five samples. By increasing the iteration times (Figs. 2C
20
21 144 and 2E), the shape of the resulting probability distribution becomes apparent
22
23 145 (Figs. 2D and 2F). We acknowledge here that more iterations will yield a more
24
25 146 accurate distribution, but will also increase computing time. A discussion on
26
27 147 how to balance the iteration time and computing resource is presented in section
28
29 148 2.4 below.
30
31
32

33 149 This approach only propagates analytical uncertainties but not uncertainties from the
34
35 150 linear regression itself. This is illustrated by the example in Figure 3. For a dataset consisting
36
37 151 of five samples that have no analytical uncertainty and do not plot on a common line (Fig. 3A),
38
39 152 using the above algorithm will result in no uncertainty for the slope and y-intercept (Fig. 3B),
40
41 153 which is not a plausible result because the fitted line does not pass through all the five samples.
42
43 154 We term these non-analytical uncertainties as the model uncertainty. The primary contributors
44
45 155 of this model uncertainty include differences in the initial isotope composition, ages, or those
46
47 156 which arise from open isotopic system behavior violating the fundamental assumptions behind
48
49 157 isochron dating. In realistic scenarios it is likely that both analytical and model uncertainties
50
51 158 will be present at some level though careful selection of samples and refined measurements
52
53 159 maybe used to minimize their effect. Using the simple Monte Carlo algorithm described above
54
55 160 which only propagates analytical uncertainties and fails to capture this extra source of
56
57
58
59
60

1
2
3 161 uncertainty. We therefore propose an extension of our method to account for this as described
4
5 162 below.

8 163 2.3 Propagation of model uncertainties

10 164 Uncertainties for the slope and y-intercept of the regression line in each sampling step
11
12
13 165 in section 2.2 (Fig. 2) are calculated as standard errors following that of James et al., (2009)
14
15 166 [29]. Further, these uncertainties are correlated as defined by the correlation coefficient (C) in
16
17
18 167 equation 1,

$$20 168 C = - \frac{\sum_{i=1}^n (x_i)}{n \times (\sum_{i=1}^n (x_i^2))^{0.5}} \quad (\text{equation 1})$$

22
23 169 where n is the number of samples (e.g., 5 for the example in Fig. 2), and x_i denotes the sampled
24
25 170 point's X-axis.

27
28 171 Knowing these uncertainties and error correlation for each sampling step, it is possible
29
30 172 to include them by replacing the outcome of each sampling step by a new probability density
31
32 173 distribution. This process is illustrated in Figure 3, where one of the outcomes from the
33
34 174 sampling step (Fig. 3B) is replaced by a new probability density distribution (Figs. 3D). For
35
36 175 input data with analytical uncertainties (Figs. 3E), when model uncertainties are included for
37
38 176 all simulations, a final distribution (blue in Fig. 3F) is obtained. This final distribution includes
39
40 177 both analytical and model uncertainties, and we term them as total uncertainties. In the presence
41
42 178 of both analytical uncertainties and model uncertainties, we cannot determine exactly whether
43
44 179 the scatter in the final distribution is inherited from analytical uncertainties or caused by model
45
46 180 uncertainties, or a combination of both.

50
51 181 Statistical analysis is applied to the final distribution to quantify the uncertainties for
52
53 182 data interpretation. We use the means and two standard deviations of the slope and y-intercept,
54
55 183 plus the correlation between them, to assess the significance of this final distribution.
56
57 184 Additionally, the contribution of analytical uncertainties to the total uncertainties (analytical +
58
59 185 model uncertainties) could be assessed. Here we emphasize that as discussed above, analytical

186 uncertainties could be an additional source of model uncertainties, hence the contribution only
187 can be assessed semi-quantitatively.

188 The advantage of this method is that regardless of the degree of fit, both analytical and
189 model uncertainties are propagated into the final distribution. In other words, the degree of fit
190 is not a prerequisite to alter the strategy of error propagation. As such, the proposed method
191 ensures that quoted uncertainties can be fairly compared as they are calculated in a consistent
192 manner.

193 2.4 The iteration times

194 To achieve a representative final distribution for the given sample set, a high number
195 of iterations are required at the expense of consuming more computing resources and time. In
196 this regard, the iteration times should be balanced between the accuracy of the final distribution
197 and the simulation time. Here we monitor the mean and standard deviation of the final
198 distribution and stop iteration once this mean and standard deviation are stabilized. Our
199 preliminary experiment suggests that an iteration count of about 10^6 is sufficient in most cases,
200 and could be increased when necessary.

201 3. Comparison with Isoplot

202 It is important to compare the results from the Monte Carlo based approach with those
203 from the Isoplot program to understand differences in the assumptions and how they propagate
204 into the resultant age estimations. In the following section, we construct a synthetic
205 experimental data set to highlight the magnitude of these differences and explore implications
206 in isochron dating.

207 3.1 Synthetic experimental dataset

208 Using the Re-Os isotopic system as an example, where ^{187}Re decays to ^{187}Os with a
209 decay constant of $1.666 \times 10^{-11} \text{ year}^{-1}$ [30, 31], we generate synthetic examples for the

210 experiment (Table 1). To be representative of geological scenarios, the examples are designed
211 to cover plausible scenarios in isochron dating, as represented by the probability of fit which
212 varies between 0 and 1 (Figure 4). For uncertainty propagation using the Isoplot program, we
213 follow the default approach in the Isoplot program to set the cut-off value as 0.15. As can be
214 seen from the following discussion, using different cut-off values should not bias our
215 conclusion. Below we outline the approaches generating these examples.

- 216 1. An age and an initial daughter isotopic ratio (i.e., $^{187}\text{Os}/^{188}\text{Os}_{\text{initial}}$) are randomly
217 assigned between 100 and 4500 Ma and 0.2–1.2, respectively, following
218 uniform distributions.
- 219 2. The number of samples, n , used to construct an isochron is randomly chosen
220 between 5 and 30 following a uniform distribution.
- 221 3. For the n samples, their parent isotopic ratios (i.e., $^{187}\text{Re}/^{188}\text{Os}$) at present day
222 are randomly selected following uniform distributions between 100 and 1000.
223 Specifically, for each example, we first randomly pick a lowest ratio and a
224 highest ratio which lie between 100 and 1000. Afterwards, we randomly pick
225 $n-2$ ratios following a uniform distribution between that lowest ratio and highest
226 ratio. The purpose of this specific approach is to guarantee that for these
227 examples, the variety of the parent isotopic ratios (spread of the isochron) in
228 each example follows a uniform distribution.
- 229 4. The daughter isotopic ratios (e.g., $^{187}\text{Os}/^{188}\text{Os}$) at present day of the n samples
230 are calculated individually following equation 2 using the t , initial daughter
231 isotopic ratio and parent isotope ratios generated in step 1, 2 and 3, respectively.
232
$$^{187}\text{Os}/^{188}\text{Os} = ^{187}\text{Os}/^{188}\text{Os}_{\text{initial}} + ^{187}\text{Re}/^{188}\text{Os} * (e^{\lambda t} - 1) \quad (\text{equation 2})$$
- 233 5. We then introduce scatter to the daughter isotopic ratios by adding or
234 subtracting a value ranging from 0.2 to 1.2 % of the corresponding daughter

1
2
3 235 isotopic ratios following uniform distributions, and the decision whether to add
4
5 236 or subtract is also random. Note that this scatter serves to imitate model
6
7 237 uncertainties. The model uncertainties are introduced through modifying the
8
9 238 daughter isotopic ratios, which cover all the potential causes of model
10
11 239 uncertainties including variations in initial isotopic composition and age, as well
12
13 240 as open system behaviour to the isotopic system and imperfect measurements.
14
15 241 6. The 2-sigma relative uncertainty (i.e., percentage uncertainty) of the parent and
16
17 242 daughter isotope ratios are randomly assigned between 0.2 and 1 % following
18
19 243 uniform distributions, with their error correlations randomly given between 0.4
20
21 244 and 0.999, which also follow uniform distributions.
22
23
24
25

26 245 The data generated above are processed by our new Monte Carlo method as well as the
27
28 246 Isoplot program. Therefore, one age and one initial isotopic composition plus their associated
29
30 247 uncertainties (2-sigma) will be obtained from the Isoplot program either following Model 1 (p
31
32 248 > 0.15) or Model 3 ($0 < p < 0.15$) solutions. For the Monte Carlo simulation, one age, one
33
34 249 initial isotopic ratio, and associated total uncertainties (analytical uncertainties+ model
35
36 250 uncertainties) are obtained for each example. We perform this process 10000 times, and as
37
38 251 expected, the probability of these examples varies between 0 and 1 with the corresponding
39
40 252 Mean Square Weighted Deviation (MSWD) ranging from >10 to 0.
41
42
43
44

45 253 3.2. Results from Monte Carlo method and the Isoplot program

46
47 254 Regardless of which linear regression tool is employed, the slopes and y-intercepts,
48
49 255 hence ages and initial isotopic ratios, are the same (Figs. 4A-D). Minimal scatter exists when
50
51 256 the spread in the synthetic data points is limited, which renders an accurate age estimation
52
53 257 difficult. Notably, uncertainties obtained from the Monte Carlo simulation are consistently
54
55 258 larger than those from the Isoplot program (Figs. 4E-5F). Here we use the $R_{MC/iso}$ to illustrate
56
57 259 these results, where $R_{MC/iso}$ equals to age uncertainties (total) from the Monte Carlo method
58
59
60

1
2
3 260 divided by age uncertainties from the Isoplot program. When p decreases from 1 to 0.15, the
4
5 261 running mean of $R_{MC/Iso}$ increases from 2 to 2.5, and indicates a progressively increasing degree
6
7 262 of underestimation of uncertainties by the Isoplot program. When p decreases from 0.15 to 0,
8
9 263 we observe a significant decrease in the running mean of the $R_{MC/Iso}$ from ~ 2 to ~ 1.5 , and then
10
11 264 gradually decrease to >1 . This relationship can further be illustrated by plotting $R_{MC/Iso}$ as a
12
13 265 function of MSWD (which is dependent on p , Fig. 4F), and shows that $R_{MC/Iso}$ reduce from 2.5
14
15 266 to 1.5 as the MSWD increases from 1.3 to 2.5, ultimately $R_{MC/Iso}$ approaches one when the
16
17 267 scatter is sufficiently large (i.e., $MSWD \gg 2.5$). A notable feature here is the abrupt change in
18
19 268 the relationship between $R_{MC/Iso}$ and probability/MSWD when p approaches 0.15. Such an
20
21 269 abrupt transition is mainly due to the contrasting error propagation strategies in Isoplot caused
22
23 270 by the utilization of an arbitrary cut-off value.

24
25
26 271 These results indicate that uncertainties following the Model 1 scenarios in the Isoplot
27
28 272 program are underestimated by 50 – 60 % compared to total uncertainties derived from the
29
30 273 Monte Carlo method (as calculated by the difference between the uncertainties relative to the
31
32 274 Monte Carlo based total uncertainties). For the Model 3 age in Isoplot, the uncertainties can
33
34 275 also be underestimated by as much as 60 %, though uncertainties become more comparable for
35
36 276 increasing MSWD.

37
38 277 An underestimation of uncertainty could be detrimental in geological studies when high
39
40 278 temporal resolution is essential. For example, when verifying the relationship between two
41
42 279 geological processes that are indistinguishable in time (e.g., 1000 ± 0.6 Ma and 999 ± 0.6 Ma),
43
44 280 an underestimation of the uncertainties by 50 % will yield ages of 1000 ± 0.3 Ma and $999 \pm$
45
46 281 0.3 Ma, which could lead to a conclusion that the two geological events were not
47
48 282 contemporaneous in time, hence rejecting a direct causal link between them. In contrast, with
49
50 283 full propagation of the uncertainties, a potential causal link cannot be ruled out.
51
52
53
54
55
56
57
58
59
60

1
2
3 284 We speculate that the underestimation of uncertainties in the Model 1 ages arises from
4
5 285 only considering analytical uncertainties without incorporating model uncertainties. This is
6
7
8 286 supported by the observations that the analytical-only uncertainties from the Monte Carlo based
9
10 287 method are comparable (though slightly larger, discussed below) to those from the Model 1
11
12 288 scenario in Isoplot program (Fig. 4G-H). The underestimation of uncertainties in the Model 3
13
14 289 ages is less transparent, but most likely due to an incomplete propagation of model
15
16 290 uncertainties.

17
18
19 291 A further feature is that when $p > 0.15$, the analytical only uncertainties from our Monte
20
21 292 Carlo method are slightly larger than those from the Model 1 solution (Figs. 4G and 4H). Such
22
23 293 a discrepancy is expected based on York et al., (2004) [24] — the uncertainties from Monte
24
25 294 Carlo method only becomes comparable with those from the least square method when
26
27 295 sampling the least-squares-adjusted data points (i.e., the projection of the observed data point
28
29 296 onto the isochron) by Monte Carlo, rather than sampling the observed data points as has been
30
31 297 done here.

32 33 34 35 36 298 **4. Potential to integrate geological information**

37
38
39 299 An additional advantage of using the Monte Carlo based method is that the resulting
40
41 300 distribution of age and initial isotopic ratios can be adjusted to integrate with geological
42
43 301 information and produce improved chronological constraints. We demonstrate this by using a
44
45 302 synthetic example consisting of 12 samples. Their $^{187}\text{Re}/^{188}\text{Os}$ and $^{187}\text{Os}/^{188}\text{Os}$ ratios and
46
47 303 associated uncertainties including error correlations (Table 2) are used to determine their age
48
49 304 and initial isotopic ratio. Results obtained from the Monte Carlo method and the algorithm of
50
51 305 the Isoplot program are presented in Figure 5. The ages and initial isotopic ratios from the two
52
53 306 methods are essentially the same (Isoplot age = 540 ± 2 Ma, initial $^{187}\text{Os}/^{188}\text{Os} = 0.600 \pm 0.013$;
54
55 307 Monte Carlo age = 540 ± 6 , initial $^{187}\text{Os}/^{188}\text{Os} = 0.600 \pm 0.063$), but uncertainties from the
56
57 308 Isoplot program are significantly smaller as discussed above. If there is evidence that these

1
2
3 309 samples are younger than 541 Ma, i.e., based on independent geological constraints, it is
4
5 310 reasonable to discard regression results that are older than 541 Ma from the final distribution
6
7 311 (Fig. 5). By doing so, the final distribution is altered, and skewed to younger ages and higher
8
9 312 initial isotopic ratios (Fig. 6). If we consider quantiles to interpret uncertainties for this
10
11 313 distribution, the age estimate changes to 539^{+2}_{-6} Ma and the initial isotopic composition to
12
13 314 $0.616^{+0.026}_{-0.035}$ at the 95% percentile level. Similarly, if the initial isotopic ratio can be
14
15
16 315 independently constrained, this information can also be integrated into the Monte Carlo method.
17
18 316 This approach is analogous to a common practice in isochron dating, where a sample or a
19
20 317 mineral containing low or negligible parent isotope is selected together with samples bearing
21
22 318 high parent isotope for isochron dating (e.g., using matrix and garnet with low and high
23
24 319 $^{176}\text{Lu}/^{177}\text{Hf}$ ratios, respectively for Lu-Hf dating; using plagioclase and pyroxene with low and
25
26 320 high $^{147}\text{Sm}/^{144}\text{Nd}$ ratios, respectively for Sm-Nd dating), through which the y-intercept of the
27
28 321 isochron is “fixed” by the sample (e.g., matrix and plagioclase) plotting near or at the y-
29
30 322 intercept. It is possible that the independent constrained geological information would also
31
32 323 have uncertainties or follow a certain distribution, these also can be considered in our Monte
33
34 324 Carlo method.

35
36
37 325 In addition, with semi-quantitatively constrained contributions of analytical
38
39 326 uncertainties to the total uncertainties, the new method provides guidance on how to yield
40
41 327 refined chronological constrains. For example, if the uncertainties are dominated by analytical
42
43 328 approaches, then improving experimental techniques would be an obvious next step to generate
44
45 329 improved chronological information. In contrast, if analytical uncertainty is not the primary
46
47 330 contributor to the total uncertainty, then the studied samples may not meet the criteria for
48
49 331 isochron dating, and better sampling strategy would be the solution for refined chronological
50
51 332 constrains.
52
53
54
55
56
57
58
59
60

333 5. Conclusions

334 A Monte Carlo based method is developed to estimate parameters (slope, y-intercept)
335 in linear regression with full propagation of their uncertainties, which is then applied to data
336 reduction for isochron geochronology. Crucially, the new method propagates both analytical
337 and model uncertainties in a consistent manner, and also allows for the user to employ *a*
338 *posteriori* geological criterion to yield refined chronological constrains and interpret the
339 significance of the analytical/model uncertainty. Using a synthetic data set, results obtained
340 from the Monte Carlo method and those from the Isoplot program are compared. The
341 comparison indicates that although the estimates of the slope (age) and y-intercept (initial
342 isotopic ratio) from both methods are similar, uncertainties following the Model 1 approach in
343 the Isoplot program are underestimated by ~60 %. For Model 3 solution in the Isoplot program,
344 the uncertainties can be underestimated by as much as 60 % depending on the goodness of fit,
345 and the results from the two methods only start to converge when the goodness of fit
346 approaches 0 (i.e., MSWD >> 2.5). We further demonstrate that geological information can be
347 integrated into our Monte Carlo based method to yield improved chronological constraints.

348 Acknowledgements

349 YL acknowledges the NERC Numerical Earth Science Modelling courses at Durham
350 University for developing coding skills, especially the help from Jeroen van Hunen and
351 Dimitrios Michelioudakis. The research is partially funded by a grant (SKL-K201706) from
352 the State Key Laboratory of Lithospheric Evolution, Institute of Geology and Geophysics,
353 Chinese Academy of Sciences. DS acknowledges the TOTAL endowment fund. ADR and YL
354 acknowledges generous funding from Yale University. The code associating this manuscript is
355 available from www.github.com/xxx.

356 **References**

- 357 1. Harrison, T. M., Baldwin, S. L., Caffee, M., et al., *It's About Time: Opportunities and*
358 *Challenges for US Geochronology*. Institute of Geophysics and Planetary Physics
359 Publication, 2015. **6539**: p. 56.
- 360 2. Ludwig, K. R., *User's manual for Isoplot 3.00: a geochronological toolkit for Microsoft*
361 *Excel*. 2003.
- 362 3. Schmitz, M. D.Schoene, B., *Derivation of isotope ratios, errors, and error correlations*
363 *for U-Pb geochronology using 205Pb-235U-(233U)-spiked isotope dilution thermal*
364 *ionization mass spectrometric data*. *Geochemistry, Geophysics, Geosystems*, 2007.
365 **8**(8): p. n/a-n/a.
- 366 4. Mattinson, J. M., *Zircon U-Pb chemical abrasion ("CA-TIMS") method: Combined*
367 *annealing and multi-step partial dissolution analysis for improved precision and*
368 *accuracy of zircon ages*. *Chemical Geology*, 2005. **220**(1-2): p. 47-66.
- 369 5. McLean, N. M., Condon, D. J., Schoene, B., et al., *Evaluating uncertainties in the*
370 *calibration of isotopic reference materials and multi-element isotopic tracers*
371 *(EARTHTIME Tracer Calibration Part II)*. *Geochimica Et Cosmochimica Acta*, 2015.
372 **164**: p. 481-501.
- 373 6. Renne, P. R., Mundil, R., Balco, G., et al., *Joint determination of 40K decay constants*
374 *and 40Ar*/40K for the Fish Canyon sanidine standard, and improved accuracy for*
375 *40Ar/39Ar geochronology*. *Geochimica et Cosmochimica Acta*, 2010. **74**(18): p. 5349-
376 5367.
- 377 7. Rivera, T. A., Storey, M., Zeeden, C., et al., *A refined astronomically calibrated*
378 *40Ar/39Ar age for Fish Canyon sanidine*. *Earth and Planetary Science Letters*, 2011.
379 **311**(3): p. 420-426.
- 380 8. Creaser, R. A., Papanastassiou, D. A.Wasserburg, G. J., *Negative Thermal Ion Mass-*
381 *Spectrometry of Osmium, Rhenium, and Iridium*. *Geochimica Et Cosmochimica Acta*,
382 1991. **55**(1): p. 397-401.
- 383 9. Völkening, J., Walczyk, T.Heumann, K. G., *Osmium isotope ratio determinations by*
384 *negative thermal ionization mass spectrometry*. *International Journal of Mass*
385 *Spectrometry and Ion Processes*, 1991. **105**: p. 147-159.
- 386 10. Jicha, B. R., Singer, B. S.Sobol, P., *Re-evaluation of the ages of 40Ar/39Ar sanidine*
387 *standards and supereruptions in the western U.S. using a Noblesse multi-collector mass*
388 *spectrometer*. *Chemical Geology*, 2016. **431**: p. 54-66.
- 389 11. Condon, D. J., Schoene, B., McLean, N. M., et al., *Metrology and traceability of U-Pb*
390 *isotope dilution geochronology (EARTHTIME Tracer Calibration Part I)*. *Geochimica*
391 *Et Cosmochimica Acta*, 2015. **164**: p. 464-480.
- 392 12. Li, X. H.Li, Q. L., *Major advances in microbeam analytical techniques and their*
393 *applications in Earth Science*. *Science Bulletin*, 2016. **61**(23): p. 1785-1787.
- 394 13. Chen, S., Wang, X., Niu, Y., et al., *Simple and cost-effective methods for precise*
395 *analysis of trace element abundances in geological materials with ICP-MS*. *Science*
396 *Bulletin*, 2017. **62**(4): p. 277-289.
- 397 14. McLean, N. M., Bowring, J. F.Bowring, S. A., *An algorithm for U-Pb isotope dilution*
398 *data reduction and uncertainty propagation*. *Geochemistry Geophysics Geosystems*,
399 2011. **12**: p. n/a-n/a.
- 400 15. McLean, N. M., Bowring, J. F.Gehrels, G., *Algorithms and software for U-Pb*
401 *geochronology by LA-ICPMS*. *Geochemistry Geophysics Geosystems*, 2016. **17**(7): p.
402 2480-2496.

- 1
2
3 403 16. Bowring, J. F., McLean, N. M. Bowring, S. A., *Engineering cyber infrastructure for U*
4 404 *-Pb geochronology: Tripoli and U-Pb_Redux*. *Geochemistry, Geophysics, Geosystems*,
5 405 2011. **12**.
- 7 406 17. Horstwood, M. S. A., Kosler, J., Gehrels, G., et al., *Community-Derived Standards for*
8 407 *LA-ICP-MS U-(Th)-Pb Geochronology - Uncertainty Propagation, Age Interpretation*
9 408 *and Data Reporting*. *Geostandards and Geoanalytical Research*, 2016. **40**(3): p. 311-
11 409 332.
- 12 410 18. Vermeesch, P., *Revised error propagation of Ar-40/Ar-39 data, including covariances*.
13 411 *Geochimica Et Cosmochimica Acta*, 2015. **171**: p. 325-337.
- 14 412 19. Dutton, A., Rubin, K., McLean, N., et al., *Data reporting standards for publication of*
15 413 *U-series data for geochronology and timescale assessment in the earth sciences*.
16 414 *Quaternary Geochronology*, 2017. **39**: p. 142-149.
- 18 415 20. Keller, C. B., Schoene, B. Samperton, K. M., *A stochastic sampling approach to zircon*
19 416 *eruption age interpretation*. *Geochemical Perspectives Letters*, 2018. **8**: p. 31-35.
- 20 417 21. Ludwig, K. R. *ISOPLOT for MS-DOS, a plotting and regression program for*
21 418 *radiogenic-isotope data, for IBM-PC compatible computers, version 1.00*. 1988. US
22 419 Geological Survey.
- 23 420 22. York, D., *Least squares fitting of a straight line with correlated errors*. *Earth and*
24 421 *Planetary Science Letters*, 1968. **5**: p. 320-324.
- 25 422 23. York, D., *Least-Squares Fitting of a Straight Line*. *Canadian Journal of Physics*, 1966.
27 423 **44**(5): p. 1079-&.
- 28 424 24. York, D., Evensen, N. M., Martinez, M. L., et al., *Unified equations for the slope,*
29 425 *intercept, and standard errors of the best straight line*. *American Journal of Physics*,
30 426 2004. **72**(3): p. 367-375.
- 32 427 25. McIntyre, G. A., Brooks, C., Compston, W., et al., *The statistical assessment of Rb-Sr*
33 428 *isochrons*. *Journal of Geophysical Research*, 1966. **71**: p. 5459-5468.
- 34 429 26. Ludwig, K. R., *Mathematical-statistical treatment of data and errors for 230Th/U*
35 430 *geochronology*. *Reviews in Mineralogy and Geochemistry*, 2003. **52**: p. 631-656.
- 37 431 27. Cumming, G. L., *A recalculation of the age of the solar system*. *Canadian Journal of*
38 432 *Earth Sciences*, 1969. **6**: p. 719-735.
- 39 433 28. Ludwig, K. R. Titterington, D. M., *Calculation of 230ThU isochrons, ages, and errors*.
40 434 *Geochimica et Cosmochimica Acta*, 1994. **58**(22): p. 5031-5042.
- 41 435 29. James, G., Witten, D., Hastie, T., et al., *An introduction to statistical learning*. Vol.
42 436 112. 2013: Springer.
- 43 437 30. Smoliar, M. I., Walker, R. J. Morgan, J. W., *Re-Os ages of group IIA, IIIA, IVA, and*
44 438 *IVB iron meteorites*. *Science*, 1996. **271**(5252): p. 1099-1102.
- 46 439 31. Selby, D., Creaser, R. A., Stein, H. J., et al., *Assessment of the 187Re decay constant*
47 440 *by cross calibration of Re-Os molybdenite and U-Pb zircon chronometers in magmatic*
48 441 *ore systems*. *Geochimica et Cosmochimica Acta*, 2007. **71**(8): p. 1999-2013.
49 442

443

444

445 Table 1, Parameters for the synthetic dataset.

Age	n	initial	X	dX	Y	dY	scatter	rho
100–4500 uniform	5–30 uniform	0.2–1.2 uniform	100–1000 uniform	0.2–1% uniform	Equation 2	0.2–1% uniform	0.2-1.2% uniform	0.4–0.999 uniform

446

447 Table 2, Re-Os data for the synthetic samples.

Sample No.	$^{187}\text{Re}/^{188}\text{Os}$	2-sigma	$^{188}\text{Os}/^{188}\text{Os}$	2-sigma	rho
Sample 1	100.000	1.540	1.504	0.023	0.936
Sample 2	200.000	2.940	2.407	0.024	0.473
Sample 3	300.000	4.830	3.311	0.037	0.764
Sample 4	400.000	3.960	4.215	0.078	0.565
Sample 5	500.000	7.150	5.118	0.057	0.635
Sample 6	600.000	10.200	6.022	0.090	0.484
Sample 7	700.000	11.620	6.926	0.082	0.949
Sample 8	800.000	12.880	7.830	0.078	0.945
Sample 9	900.000	12.780	8.733	0.096	0.910
Sample 10	1000.000	10.900	9.637	0.165	0.994
Sample 11	1100.000	19.580	10.541	0.065	0.477
Sample 12	1200.000	7.440	11.444	0.161	0.452

448

449

1
2
3 450 *Figure 1, Data and uncertainties with associated error correlations (ρ) are presented as*
4
5 451 *error ellipse and error bar (A) as well as probability density function (B). The plots show*
6
7 452 *the same data and their uncertainties (cross hairs) and only vary in their correlation*
8
9 453 *(values are indicated on each plot). All uncertainties are presented at the 2-sigma level*
10
11 454 *(95.45% confidence).*
12
13
14
15 455

16
17 456 *Figure 2, The principle of the Monte Carlo based simulation is illustrated by an example*
18
19 457 *comprising five samples. A) Randomly sampling a data point from the PDFs of each of the*
20
21 458 *five samples and estimating its slope and y-intercept using the simple least-squares method.*
22
23 459 *The slope and y-intercept from A are plotted in B. C-D) 10 and E-F) 1000 iterations of the*
24
25 460 *procedure described for panels A and B. The accuracy of the final distribution (F)*
26
27 461 *improves with increasing iterations / sampling.*
28
29
30
31 462

32
33 463 *Figure 3, The presence of model uncertainties. As illustrated by a synthetic example*
34
35 464 *comprising five samples not plotting on a line, assuming no analytical uncertainties (A),*
36
37 465 *sampling according to their PDFs will yield a distribution without uncertainties (B)*
38
39 466 *although in fact it has uncertainty. This indicates the presence of non-analytical*
40
41 467 *uncertainties, which are defined as model uncertainties and need to be accounted for.*
42
43 468 *Using the same samples without analytical uncertainties (B), the model uncertainty has*
44
45 469 *been illustrated by a new distribution in blue (C). A more realistic data set, in which data*
46
47 470 *have analytical uncertainties (E), model uncertainties have been added to all resampled*
48
49 471 *regressions, a final distribution (blue points) is obtained (F) which includes both analytical*
50
51 472 *and model uncertainties.*
52
53
54
55
56 473
57
58
59
60

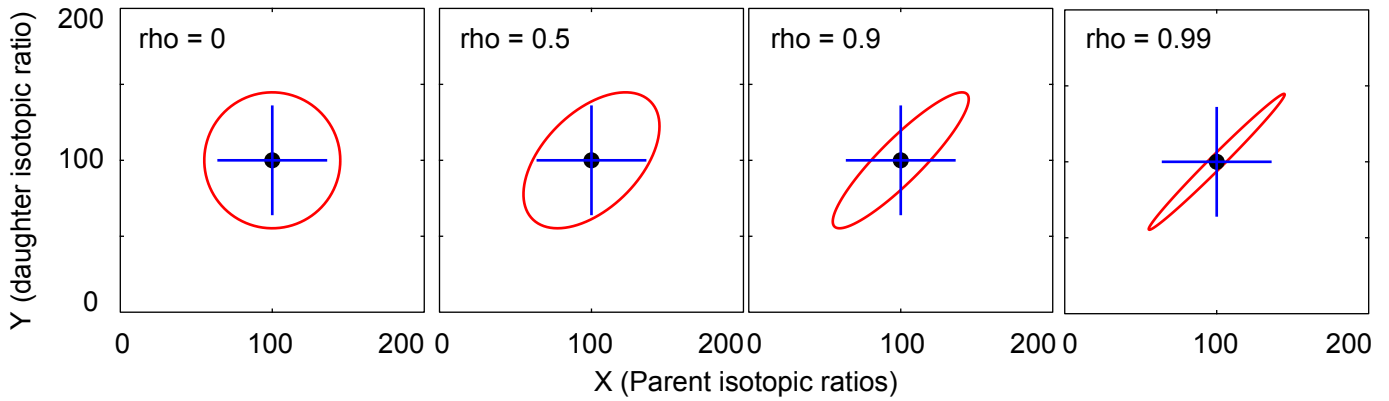
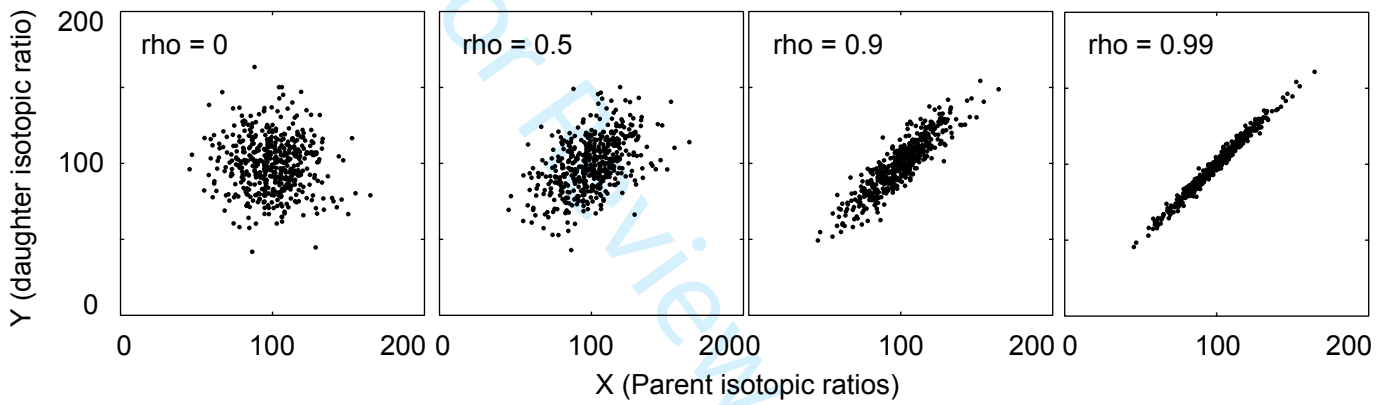
1
2
3 474 *Figure 4, Comparison results from Isoplot and Monte Carlo methods using synthetic examples.*

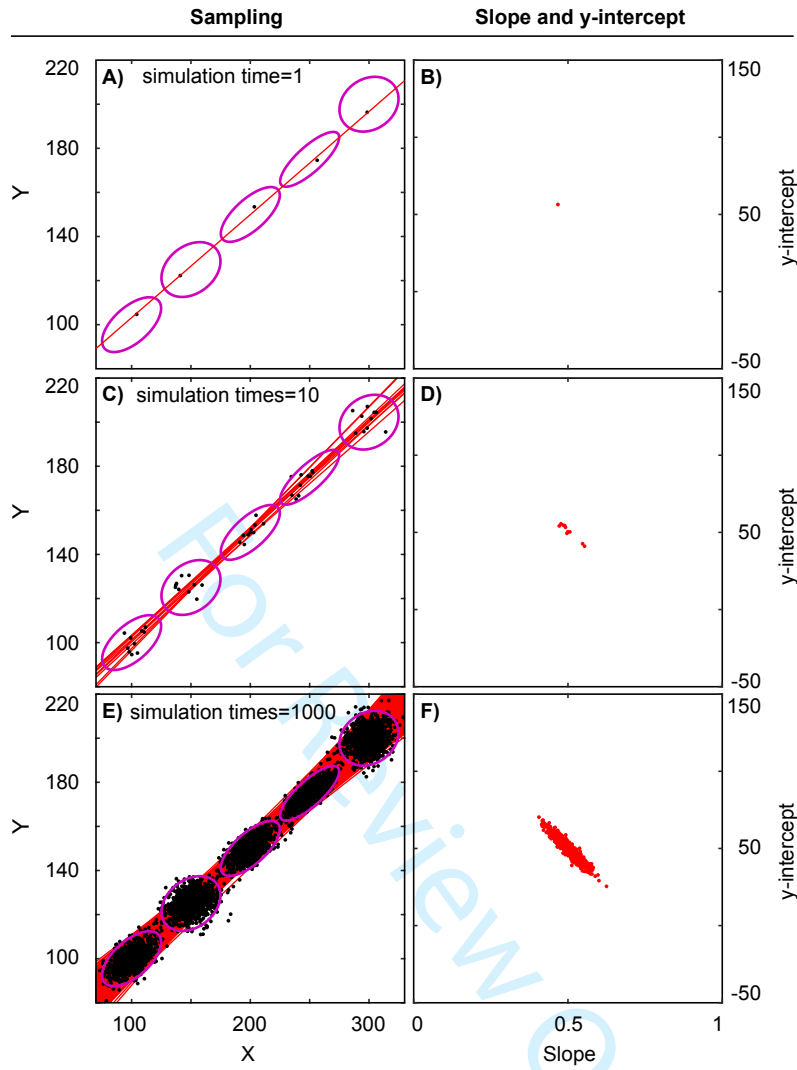
4
5 475 *Note for uncertainties from Monte Carlo method and Isoplot program, their relationship*
6
7
8 476 *has an abrupt change at $p=0.15$, likely due to the contrasting strategies of error*
9
10 477 *propagation in Model 1 and Model 3 solutions. Comparison of the slope estimate as a*
11
12 478 *function of the probability of fit (A) and MSWD (B) and y-intercept estimate as a function*
13
14 479 *of the probability of fit (C) and MSWD (D). The slope and y-intercept estimates, hence age*
15
16 480 *and initial isotopic ratio estimates, from the two methods are comparable. In cases when*
17
18 481 *the analytical and model uncertainties are taking into account (E, F), the uncertainties of*
19
20 482 *the slopes and y-intercepts from the Monte Carlo based simulation are larger than those*
21
22 483 *from the Isoplot program. When only the analytical uncertainties are considered (G, H),*
23
24 484 *the Isoplot Model 1 age uncertainty is comparable but slightly larger than the Monte Carlo*
25
26 485 *based approach.*

27
28
29
30
31 486
32
33 487 *Figure 5, Re-Os chronological results of the 12 synthetic samples using the Monte Carlo based*
34
35 488 *method and the Isoplot program. A), Isochron diagram using the algorithm of the Isoplot*
36
37 489 *program; B), Analytical only and analytical + model uncertainties obtained from the*
38
39 490 *Monte Carlo method at the 2-sigma level; C), The final distribution of age and initial*
40
41 491 *isotopic composition visualized by the Monte Carlo based method.*

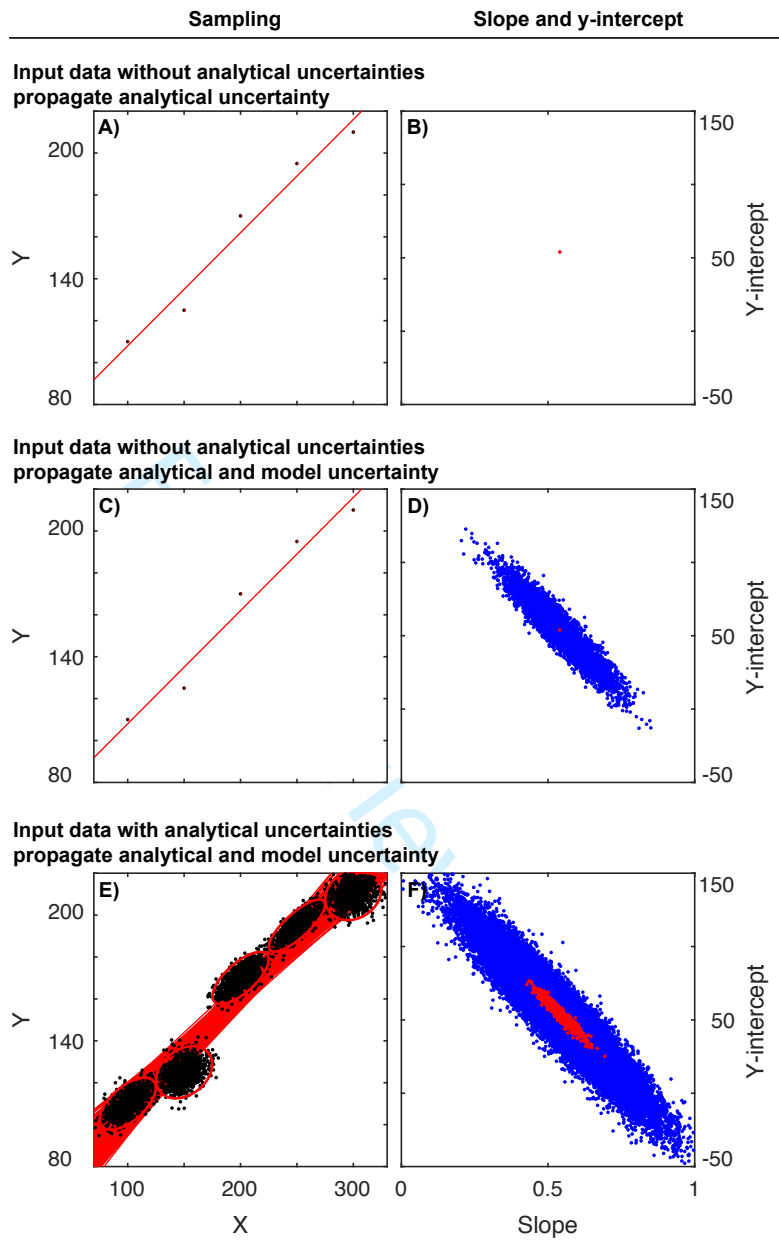
42
43
44 492
45
46
47 493 *Figure 6, Improving chronological constraints through integrating geological information for*
48
49 494 *the synthetic example in Figure 5. In this example, we assume that the samples are younger*
50
51 495 *than 541 Ma, and hence simulation results larger than 541 Ma are removed to yield a*
52
53 496 *better constrained chronological result.*

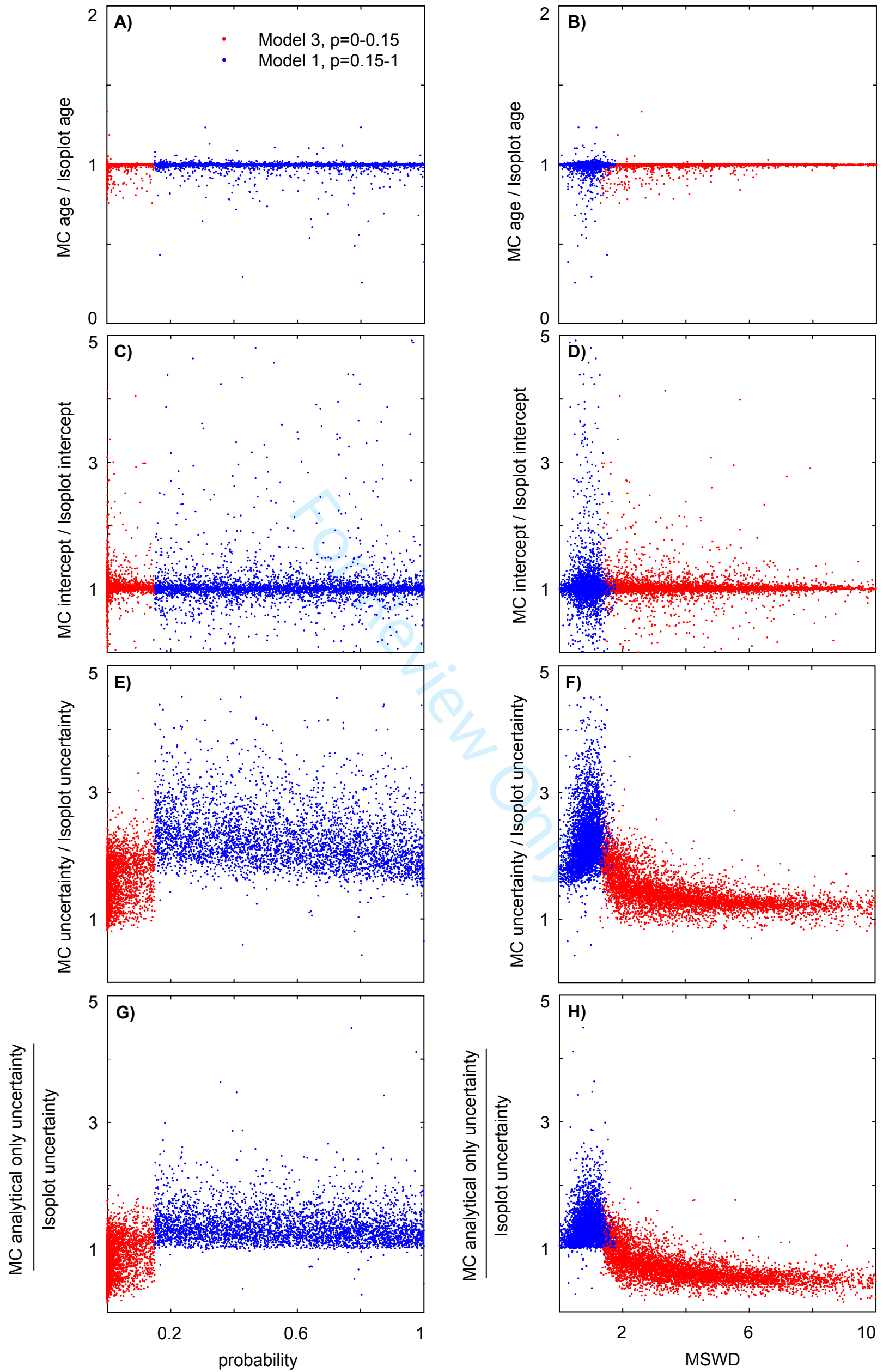
54
55
56 497
57
58
59
60

A) Error bar and error ellipse**B) Probability density function**



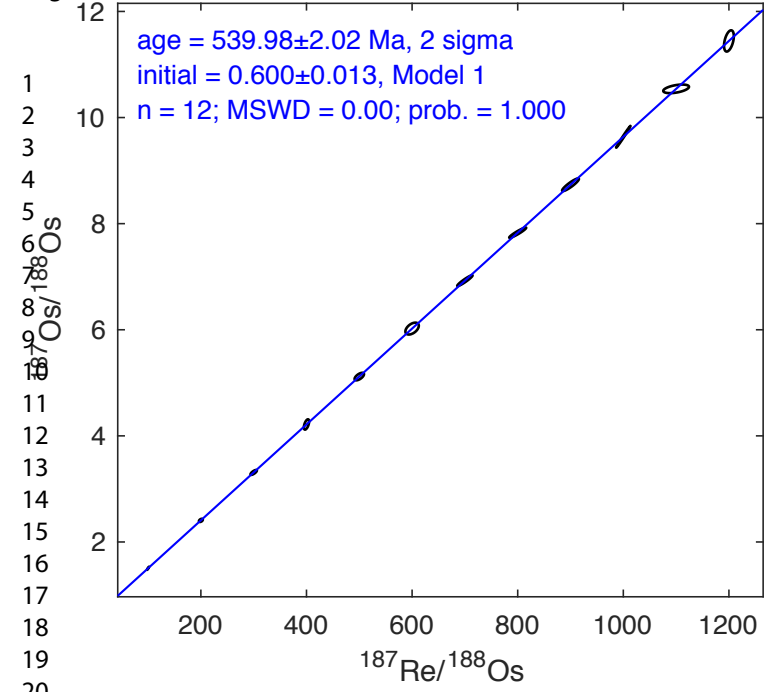
1
2
3
4
5
6
7
8
9
10
11
12
13
14
15
16
17
18
19
20
21
22
23
24
25
26
27
28
29
30
31
32
33
34
35
36
37
38
39
40
41
42
43
44
45
46
47
48
49
50
51
52
53
54
55
56
57
58
59
60



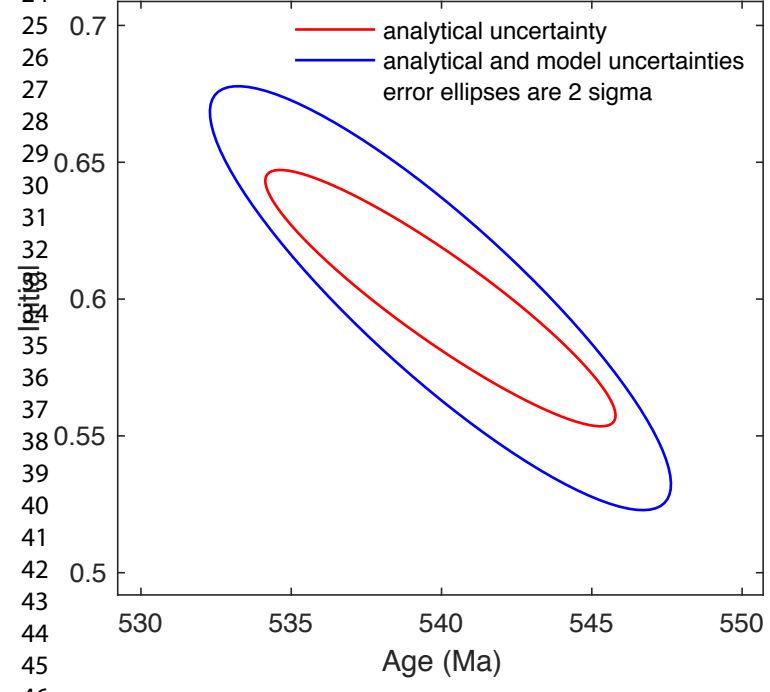


1
2
3
4
5
6
7
8
9
10
11
12
13
14
15
16
17
18
19
20
21
22
23
24
25
26
27
28
29
30
31
32
33
34
35
36
37
38
39
40
41
42
43
44
45
46
47
48
49
50
51
52
53
54
55
56
57
58
59
60

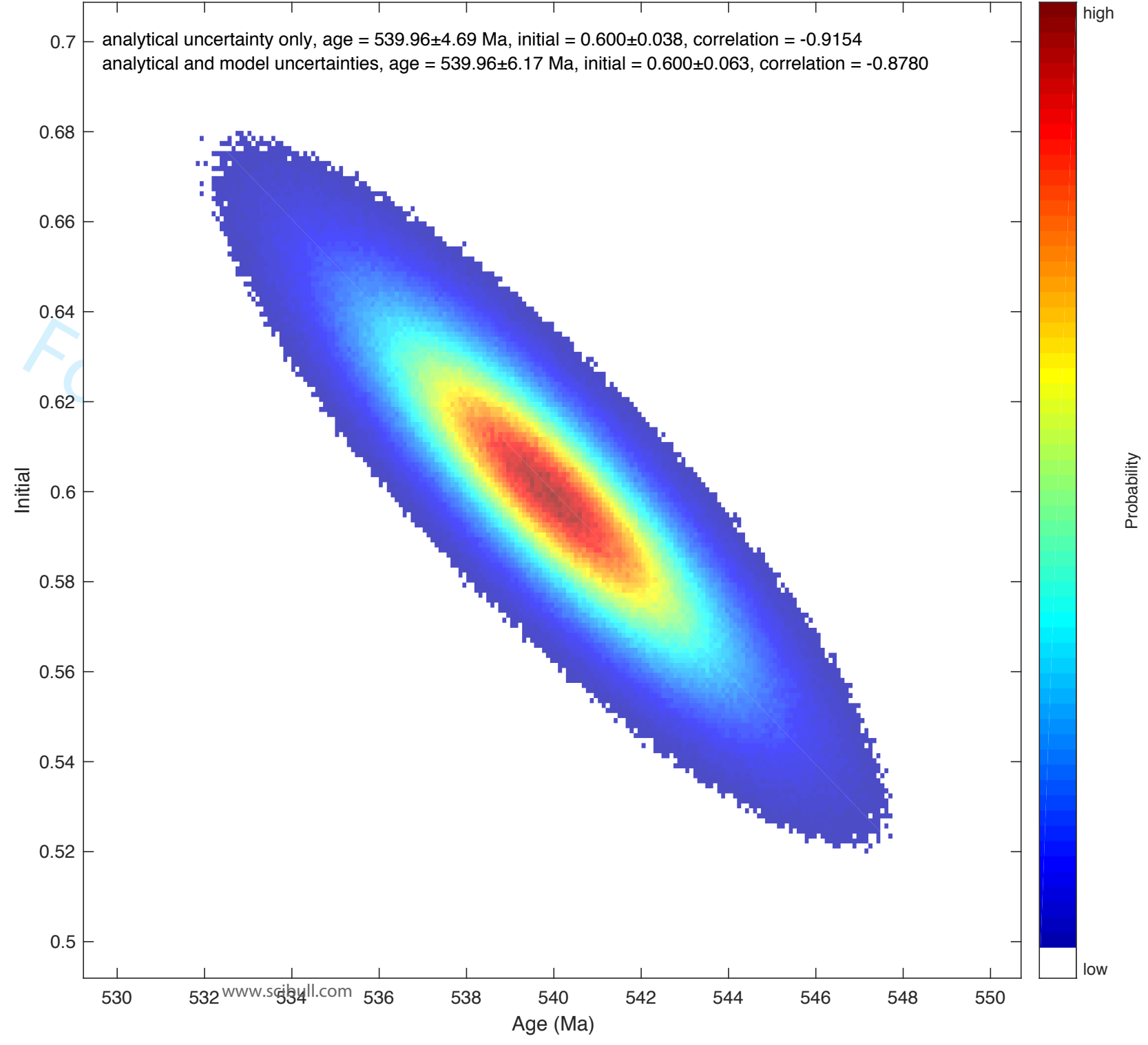
A) Ludwig Isoplot Isochron



B) Uncertainties from Monte Carlo simulation



C) Contour plot of Monte Carlo simulation



C) Contour plot of Monte Carlo simulation

